Supporting Information for

Gate-Controllable Quadri-Layertronics in 2D Multiferroic Antiferromagnet

Ting Zhang,[1*] Mingsheng Wang,[1] Xilong Xu,[2] Ying Dai,[3] Yandong Ma[3*]

[1]School of Physics and Technology, University of Jinan, Jinan 250022, People's Republic of China

[2]Department of Physics, Washington University in St. Louis, Missouri 63130, USA

[3]School of Physics, Shandong University, Jinan 250100, People's Republic of China

*Corresponding author: sps_zhangt@ujn.edu.cn (T.Z.); yandong.ma@sdu.edu.cn (Y.M.);

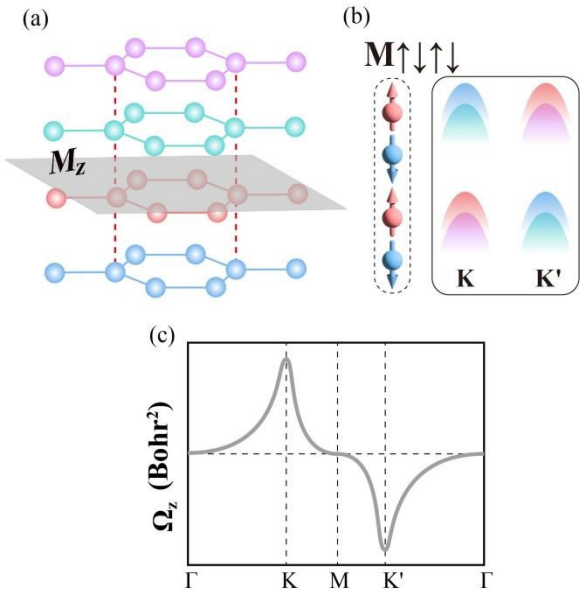

Fig. S1 (a) Crystal structures, (b) band structure and spin direction, and (c) Berry curvatures of the AAAA configuration of quadrilayer lattice with M_z symmetry.

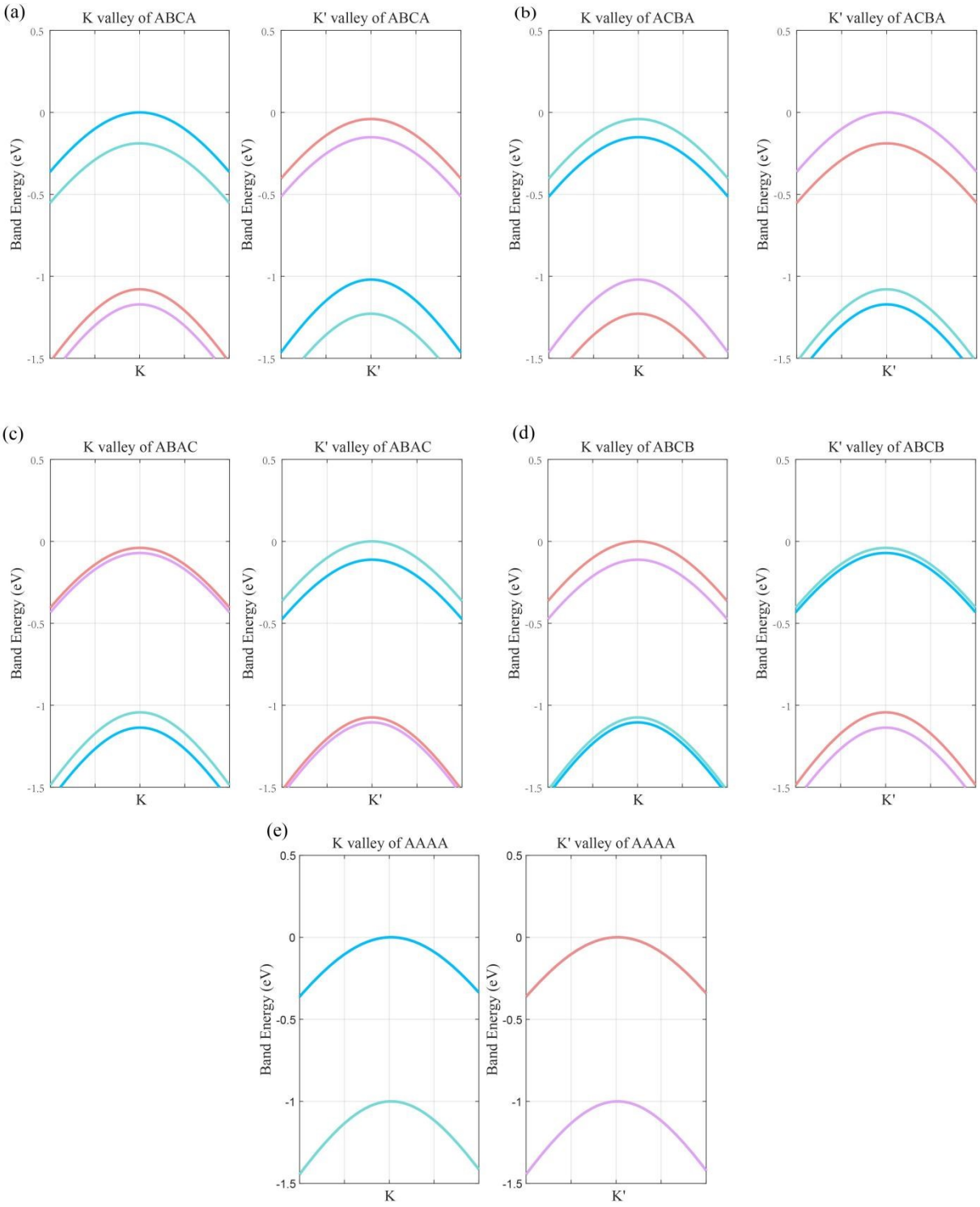

Fig. S2 Low-energy band dispersions near the K and K' valleys based on the $k \cdot p$ model for the (a) ABCA, (b) ACBA, (c) ABAC, (d) ABCB and (e) AAAA configurations of quadrilayer lattice.

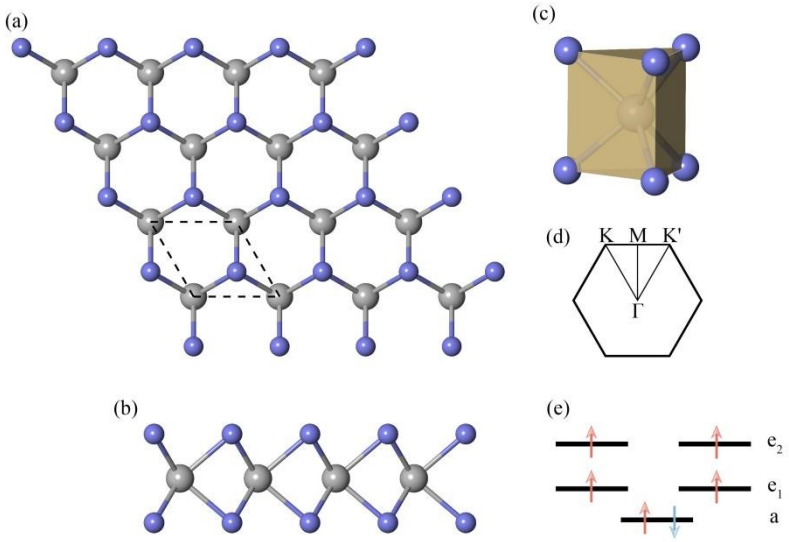

Fig. S3 (a) Top view and (b) side view of single-layer $OsCl_2$, where the dashed box in (a) represents the unit cell, and the balls of blue and gray label the Cl and Os atoms, respectively. (c) Coordinate atom around Os atom constituting the local structure of $OsCl_6$. (d) The first Brillouin zone. (e) Schematic illustration of energy level splitting of *d* orbitals caused by trigonal prism crystal field, the distribution of six *d* electrons of cation Os in energy level shows a high-spin state.

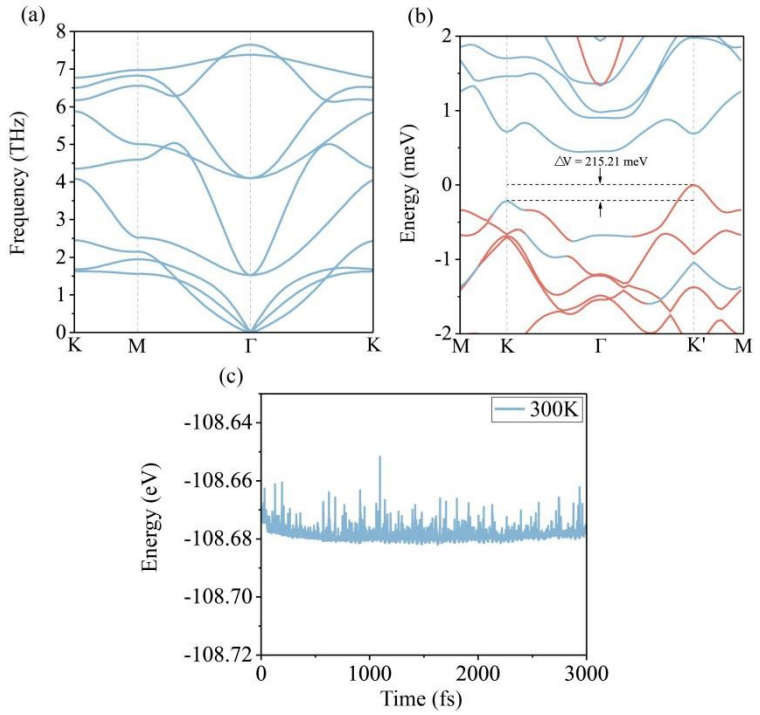

Fig. S4 (a) Phonon spectrums of single-layer $OsCl_2$. (b) Band structures of single-layer $OsCl_2$ with SOC. Blue and red lines represent the spin-down and spin-up states. (c) Evolution of the total energy from the 3 ps AIMD simulation at 300 K.

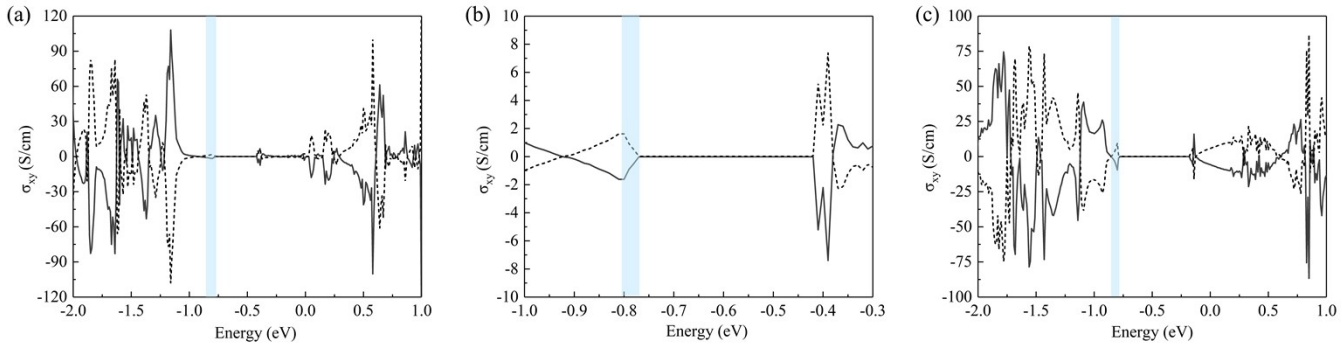

Fig. S5 (a) Anomalous Hall conductivity of the ABCA (solid line) and ACBA (dotted line) stacking configurations. (b) A magnified view of panel (a) focusing on the valence band edge near the Fermi level. (c) Anomalous Hall conductivity of the ABCB (solid line) and ABAC (dotted line) configurations.

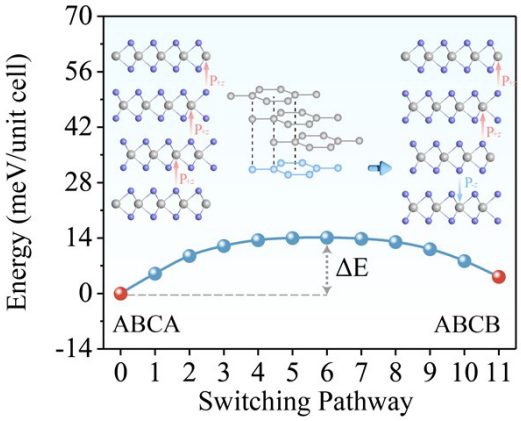

Fig. S6 Energy profiles for ferroelectric switching between ABCA and ABCB configurations in quadrilayer $OsCl_2$.

Table S1. Energy differences between FM and AFM states and magnetocrystalline anisotropy energy of ABCA, ACBA, ABAC, and ABCB configurations of quadrilayer $OsCl_2$.

	QL-FM (eV/cell)	QL-AFM (meV/cell)	MAE (eV/cell)
ABCA (ACBA)	0.031	0	0.13
ABAC (ABCB)	0.023	0	0.03

Methods

First-principles calculations are performed based on density functional theory (DFT) as implemented in the Vienna ab initio simulation package (VASP)[1,2]. The exchange-correlation interaction is treated by the generalized gradient approximation (GGA) in the form of Perdew, Burke, and Ernzerhof (PBE) functional[3]. The convergence criteria for energy and force are set to 10^{-5} eV and 0.01 eV $Å^{-1}$. The cutoff energy is set to 500 eV. A 13 × 13 × 1 Monkhorst-Pack grid is adopted for k-point sampling. Considering the strong correlations, we use the GGA + *U* approach with $U_{eff} = (U - J) = 2$ eV for Os-*d* orbital according to previous work[4]. Grimme's DFT-D3 method[5] is included to describe the van der Waals interaction. The Berry curvature is calculated using VASPBERRY[6]. The ferroelectric polarization is evaluated using the Berry phase approach[7], and the energy barrier of ferroelectric switching is obtained by nudged elastic band (NEB) method[8].

References

1. Kresse, G. & Furthmüller, J. Efficient Iterative Schemes for ab Initio Total-Energy Calculations using a Plane-Wave Basis *Set. Phys. Rev. B* 54, 11169-11186 (1996).

2. Kohn, W. & Sham, L. Self-Consistent Equations including Exchange and Correlation Effects. *Phys. Rev.* 140, A1133-A1138 (1965).

3. Perdew, J., Burke, K. & Ernzerhof, M. Generalized Gradient Approximation Made Simple. *Phys. Rev. Lett.* 77, 3865-3868 (1996).

4. Xie, W., Zhang, L., Yue, Y., Li, M. & Wang, H. Giant Valley Polarization and Perpendicular Magnetocrystalline Anisotropy Energy in Monolayer MX2 (M = Ru, Os; X = Cl, Br). *Phys. Rev. B* 109, 024406 (2024).

5. Grimme, S., Ehrlich, S. & Goerigk, L. Effect of the Damping Function in Dispersion Corrected Density Functional Theory. J. *Comput. Chem.* 32, 1456-1465 (2011).

6. Fukui, T., Hatsugai, Y. & Suzuki, H. Chern Numbers in Discretized Brillouin Zone: Efficient Method of Computing (Spin) Hall Conductances. *J. Phys. Soc. Jpn.* 74, 1674-1677 (2005).

7. King-Smith, R. & Vanderbilt, D. Theory of Polarization of Crystalline Solids. *Phys. Rev. B* 47, 1651-1654 (1993).

8. Henkelman, G., Uberuaga, B. & Jónsson, H. A climbing Image nudged Elastic Band Method for finding Saddle Points and Minimum Energy Paths. *J. Chem. Phys.* 113, 9901-9904 (2000).